

See discussions, stats, and author profiles for this publication at: <http://www.researchgate.net/publication/277255360>

An Experimental and Multiphysics Based Numerical Study to Predict Automotive Fuel Tank Sloshing Noise

CONFERENCE PAPER · APRIL 2014

DOI: 10.4271/2014-01-0888

DOWNLOADS

17

VIEWS

24

8 AUTHORS, INCLUDING:



[R. Banerjee](#)

Indian Institute of Technology Hyderabad

25 PUBLICATIONS 67 CITATIONS

SEE PROFILE



An Experimental and Multiphysics Based Numerical Study to Predict Automotive Fuel Tank Sloshing Noise

2014-01-0888
Published 04/01/2014

V. Jadon, G. Agawane, A. Baghel, Venkatesham Balide, and R. Banerjee
IIT Hyderabad

A. Getta, H. Viswanathan, and A. Awasthi
Mercedes Benz R&D India

CITATION: Jadon, V., Agawane, G., Baghel, A., Balide, V. et al., "An Experimental and Multiphysics Based Numerical Study to Predict Automotive Fuel Tank Sloshing Noise," SAE Technical Paper 2014-01-0888, 2014, doi:10.4271/2014-01-0888.

Copyright © 2014 SAE International

Abstract

With significant decrease in the background noise in present day automobiles, liquid slosh noise from an automotive fuel tank is considered as a major irritant during acceleration and deceleration. All major international OEMs and their suppliers try to reduce sloshing noise by various design modifications in the fuel tank. However, most major activities reported in open literature are primarily based on performing various CAE and experimental studies in isolation. However, noise generation and its propagation is a multiphysics phenomenon, where fluid mechanics due to liquid sloshing affects structural behaviour of the fuel tank and its mountings which in turn affects noise generation and propagation. In the present study a multiphysics approach to noise generation has been used to predict liquid sloshing noise from a rectangular tank. Computational Fluid dynamics (CFD), Finite Element Analysis (FEA) and Boundary Element Method (BEM) simulation studies have been performed in a semi-coupled manner to predict noise. VOF based multiphase model along with $k-\epsilon$ turbulence model was used to perform the CFD studies. Sloshing Noise generated due to fluid interaction with structural walls is simulated using Vibro-acoustic model. An integrated model is developed to predict dynamic forces and vibration displacement on tank walls due to dynamic pressure loading on tank walls. Noise radiated from tank walls is modelled by Harmonic Boundary Element Method. Experimental and numerical studies have been performed to understand the mechanics of sloshing noise generation. Images from high speed video camera and noise measurement data have been used to compare with numerical models.

Introduction

Liquid fuel in a partially filled automotive tank oscillates when subjected to sudden acceleration or deceleration. This is called liquid sloshing and is a source of noise generation in an automobile. Due to sloshing, complex surface waves are

generated and dynamic forces are exerted on the tank walls. This results in noise generation which is typically referred as sloshing noise. Due to dramatic minimization of other sources of noise generation in an automobile like engine, exhaust, tyre and air-borne noise, noise generation due to sloshing in the fuel tank is getting increased attention as it is considered to be an irritant for the passenger in the vehicle.

Based on their experimental work, Wachowski et al [1] classified sloshing noise into three categories: Splash, Hit and Clonk noise. Each of these three categories of noise occur at distinct range of frequencies. Wiesche [2] derived a correlation between slosh noise pressure fluctuations within the sloshing liquid. He used two-phase Computational Fluid Dynamics (CFD) to track liquid interface within realistic tank geometries to determine these pressure fluctuations. Kamei et al [3] also determined a sloshing noise correlation that relates factors pertaining to the fuel tank, body parts and tank mounting structure. The tank mounting structure which is related to both the fuel tank and the body parts has the largest contribution to sloshing noise.

Stedtnitz and Appel [4] reported one of the earliest work related to liquid sloshing and the dynamic force generation for automotive applications. However, their work was restricted to a spring-mass and pendulum based lumped-parameter analysis. However in recent years various Computer Aided Engineering (CAE) tools are being used to study fuel sloshing and noise generation. Kamiya et al [5] used coupled analysis to study interaction between fluid and structure models to predict sloshing. IU et al [6] used CFD to determine mean and turbulent kinetic energy and used this data to compare sound measurements. Roh et al [7] compared CFD simulations with flow visualization experiments in a transparent tank. Impact pressure on tank wall was used to determine noise source on the wall. Di Matteo et al [8] performed CFD and experimental studies to determine liquid sloshing characteristics during a

prescribed sequence of oscillations. Wasfy et al [9] used time-accurate finite element code that solves turbulent Navier Stokes equation along with a series of equations that solves multibody dynamics. Chitkara et al [10] have used CFD code to visualize study liquid sloshing in a tank for various fill levels. De Man and Van Schaftingen [11] performed a source-path-receiver analysis for both structural and air borne noise for a sloshing fuel tank.

The above literature survey shows that only one or two CAE based tools have been used to study liquid sloshing. However, sloshing inside a tank is a multi-physics problem as liquid oscillations excites the tank walls which in turn radiates noise externally. Very few studies have used a multi-physics approach to determine sloshing noise. Li et al [12] used CFD, Finite Element and Acoustic simulation methods to estimate radiated fuel slosh noise. Park et al [13] used a Fluid Structure Interaction (FSI) approach to predict noise due to sloshing. Vyta and Ando et al [14] performed a one-way coupled FSI analysis. They studied the effect of deceleration magnitude for different fuel tank fill level.

It is still well accepted that the mechanics of noise generation due to sloshing is not well understood. However, slosh noise prediction and its prevention is important from fuel tank design point of view. Therefore in this work an attempt has been made to determine the efficacy of one-way coupled CFD, FEA and Acoustic modelling as an effective tool for slosh noise prediction. Preliminary studies have been performed with this multiphysics approach and results were compared with corresponding experiments. The rest of the paper will describe in detail the experimental setup, the numerical formulation and the validation of the multi-physics CAE approach to predict slosh noise for two different fill levels in a rectangular tank.

Experimental Setup

Figure 1 shows the schematic diagram of the sloshing noise experiment, which simulates the sloshing phenomenon under control braking load to measure dynamic force and dynamic acceleration on the tank wall. It also measures sloshing noise radiated from the tank. The system consists of four major subsystems which are loading mechanism, braking mechanism, rectangular tank with provision for sensor mounting and vehicle travel track. The vehicle is accelerated when a dead weight falls due to gravity and the vehicle is attached to the dead weight by a string and pulley mechanism. A band brake is used to apply the brake. The liquid inside the tank sloshes due to the sudden application of this brake. Different sensors are mounted on the vehicle to record the effect of this sloshing activity.

The required acceleration and deceleration are estimated from equations (1a) and (1b) respectively,

$$a = \frac{m_2 g - \mu m_1 g}{m_1 + m_2}$$

1 (a)

$$d = \left(\frac{t_1}{t_2} \right) \left(\frac{m_2 g - \mu m_1 g}{m_1 + m_2} \right)$$

1 (b)

where, m_1 is the mass of the tank with water, m_2 is the mass of the dead weight, a is the acceleration of the tank, d is the deceleration of the tank, t_1 is the time required to reach the required acceleration, t_2 is required time for deceleration, and μ is coefficient of friction.

A transparent rectangular tank made of Acrylic was fabricated with a length of 238 mm, width of 220 mm and height of 238 mm. The tank wall was 6 mm thick. This tank was placed over a wooden platform that was attached to quieter wheels in order to reduce background noise. The tank and the carriage is referred as a vehicle in the rest of this paper. The platform was maintained at a horizontal position with respect to the ground with the help of a spirit level. A three axis linear inertia acceleration sensor (3g-ADXL335) and a line triggering sensor were mounted on this platform. The inertia sensor used to monitor vehicle acceleration and deceleration. An aluminum track of approximately 1.5 m was prepared on which the vehicle would travel. Special care was taken to minimize lateral movement of the vehicle.

Dynamic force sensor (Dytran 1053V3, Dytran 1051V4) and dynamic acceleration sensor (Dytran 3055B1) were mounted on the tank walls. Depending on the experimental condition, the sensors can be mounted at 10%, 30%, 50% and 70% of tank height as shown in figure 2. Noise radiated due to liquid sloshing inside the tank was monitored using four microphones that were placed in front, left, right and top direction of the tank at a distance of 0.5 m from the final resting position of the tank wall. Data from all sensors were acquired using a NI cDAQ-9178 data acquisition system which was triggered by the line sensor, which is in turn was activated by the color change in the vehicle track. A customized Labview program was used to acquire the data from all the sensors. Phantom V12.1 high speed camera was used to capture the liquid sloshing behavior, which was also triggered by the line sensor. Various camera settings were used to acquire the video. The present work reports the images that were obtained with a camera frame rate of 5000 fps. An extensive study was conducted to determine repeatability of the test data. Parametric studies were conducted with varying fill levels and sensor locations.

Numerical Formulation

This section describes the mathematical formulation and philosophy for one way coupled slosh noise prediction.

CFD Modeling

Time accurate multiphase CFD modelling was used to track the liquid surface when the tank was subjected to a transient axial acceleration and deceleration. The numerical method used in the present work is a finite volume method that solves the integral form of governing equations. In this method the

governing equations are integrated over a control volume enclosed by a control surface. Commercial CFD software Star CCM+ v7.4 [15] was used in this study.

The Volume of Fluid (VOF) method was used to track and locate the free surface motion during liquid sloshing in the tank. The VOF method adopts volume fraction as the variable for spatial distribution of each phase at a given time instant. Volume Fraction of a phase can be defined in terms of the ratio of the volume occupied by the i^{th} phase to the computational cell volume. The interface is tracked by solving continuity equation for the volume fraction of phases. For the i^{th} phase the VOF formulation is given as,

$$\frac{d}{dt} \int_V \alpha_i dV + \int_S \alpha_i v \cdot dS = 0$$

2

where, $\alpha_i = V_i / V$, V is the volume of the computational cell, S is the surface area of the computational cell normal to the velocity vector v .

The VOF model assumes that velocity, pressure, and temperature fields are shared by all immiscible fluid phases present in a control volume. The equations describing mass, and momentum are solved in the same way as it is solved for single phase flow but for an equivalent fluid whose physical properties are calculated as a function of the volume fraction of the constituent phases in the computational cell. The transport properties like density and viscosity are given as,

$$\rho = \sum_i \rho_i \alpha_i$$

$$\mu = \sum_i \mu_i \alpha_i$$

3

where, ρ_i and μ_i is the density and viscosity of the i^{th} phase. The sum of volume of fractions of all the phases in any given computational cell is unity.

While using the VOF model, only one single momentum equation is solved. The Navier Stokes equations are solved using the Segregated Flow model. It is solved on a collocated grid and the Rhie-Chow Interpolation is used for pressure-velocity coupling. The linear flow equations are solved using the initial mass flux and pressure field, which gives the intermediate velocity field. The pressure correction equation is subsequently solved to determine the corrected pressure field, which in turn is used to determine the corrected velocity field. The continuity equations is of the form

$$\frac{d}{dt} \int_V \rho dV + \int_S \rho v \cdot dS = 0$$

4

The momentum equation is given as,

$$\frac{\partial}{\partial t} \int_V (\rho v dV) + \int_V \rho v \cdot dS = - \int_S p l \cdot dS + \int_S T \cdot dS + \int_V \rho b dV$$

5

As the flow is highly turbulent, Realizable two layer k- ϵ turbulence model was used. This model combines the Realizable k- ϵ model with the two layer approach. After getting corrected velocity field from the momentum equation, equations for volume fraction and k- ϵ model are solved. The whole process moves to next time step when residual of all the equations included in this process is reduced to a defined level.

Acoustic Modeling

Figure 3 shows the philosophy of slosh noise simulation. Based on the structural flexibility of the wall, the problem can be solved either as one-way coupled or two-way coupled FSI problem. This can be used to determine the dynamic pressure and corresponding wall displacement. This vibration displacement acts as a boundary condition in the acoustic analysis. Similarly, in acoustic analysis the tank can be modelled as acoustically rigid or flexible. If the tank is acoustically flexible, then it can be modelled as acoustic-structural coupled problem.

Figure 4 shows the one-way coupled approach for noise generation in time and frequency domain. Displacement in time domain is determined by applying a transient pressure on structural wall. Similarly, using Fast Fourier Transform (FFT) on transient pressure data from CFD, pressure in frequency domain is determined. It is applied as excitation to the structural wall and corresponding harmonic displacement is calculated by doing harmonic FEM analysis. These displacements are used as acoustic boundary conditions in corresponding acoustic transient BEM and acoustic harmonic BEM analysis. Propagating sound pressure level is determined at defined field point locations

As mentioned before, noise generated due to liquid sloshing is categorized into three types of noise sources, which are Clonk, Hit and Splash Noise. Clonk and Hit noise dominates the frequency range of 50 Hz to 2000 Hz and Splash noise is dominants in the higher frequency range of 500 to 10 kHz range. The splash noise is due to the liquid-liquid interaction. The current proposed Vibro-acoustic model will not compute splash noise.

The frequency domain approach can be performed by taking pressure loading on tank walls from computational fluid dynamics (CFD) study. This approach is valid for linear sloshing regime where it is assumed that the change in the liquid center of gravity is negligible. However, it may not be true for higher deceleration loading. Hence, it is required to consider a time domain approach for nonlinear sloshing. Nonlinear sloshing predominates for higher deceleration

loading or higher fill levels. The current analysis assumes that the tank walls are acoustically rigid and therefore one-way coupling was considered.

The numerical method used for acoustic analysis is a boundary element method that solves Kirchoff-Helmholtz integral equations with normal surface vibration velocity as boundary conditions. Boundary element method reduces complex three-dimensional geometry to two-dimensional surface and only discretization of boundary is sufficient in these methods. Basis functions are selected in such way that it should satisfy the governing partial differential equation. Undetermined coefficients are estimated by satisfying the boundary conditions. This method can be used for internal and external sound radiation problems. Commercial acoustic software LMS Virtual Lab [16] is used in this study.

Results and Discussion

Experimental Results

Figures 5 and 6 shows the experimental test result data for 20% and 60% fill conditions, respectively. The dead weight mass was so adjusted such that a deceleration of 0.25 g was obtained. The sensors were placed at a height of 10 percent below the fill level. Each experiment was repeated at least three times on different days to ensure repeatability and reproducibility. The figures show the recorded test data of inertia acceleration in three directions, dynamic force and acceleration on the tank wall in the front and back directions of vehicle motion direction, sound pressure level at 0.5 m distance in front, left, right and top directions of the tank as a function of time. It is observed from the inertia acceleration sensor data that acceleration in a downward direction (Z direction) is 1 g and is constant with time. Lateral acceleration (Y) is less than 0.1 g and therefore negligible. In vehicle moving direction the braking events starts after 0.99 second. A deceleration of 0.25 g is achieved for a duration of 0.5 second. After the braking event, the change in dynamic force, dynamic acceleration and sound pressure level were synchronously observed. So, current experimental setup is able to capture major events during sloshing effectively.

The peak response of the dynamic force in front and back direction is out of phase. It is observed from the high speed camera images that due to forward motion of the fluid after the application of brake, the liquid recedes from the rear wall. Therefore when a peak in the dynamic force is observed at the front wall, a trough is noted at the rear wall. Similarly, when the liquid sloshes back to the rear wall, there is a rise in the dynamic force at the rear wall with a corresponding decrease at the front wall. This periodic motion at the rate of sloshing period continues till the liquid comes to a rest. The dynamic force response and tank wall accelerations are related and the trend is similar. The peak sound pressure level in noise measurement is associated with a peak response in acceleration and force and happens at the same time. It can be concluded that noise radiation from tank has a strong

correlation with dynamic force and acceleration response. Peak responses in measured parameters get damped with time.

Numerical Analysis

A 3D geometry was created with a dimension similar to the tank used in the experimental studies. Three different grids were created: 32×32×32, 64×64×64 and 128×128×128. A grid independence study was performed where the performance of all the three grids was evaluated with respect to the pressure time history. As can be seen in figure 7 (a), all the grids give a very similar profile. However, the computational time required for the finest grid was extremely large and therefore 64×64×64 was used for all the CFD simulations. To analyze the sensitivity of the numerical solution to time step size, three different time step size was analyzed: 10⁻³, 10⁻⁴ and 10⁻⁵ second. The results are plotted in figure 7 (b) and as can be seen from the plot, the pressure time history for 10⁻⁴ and 10⁻⁵ are very close. However, the simulation time with 10⁻⁵ second is very high. Therefore, all the results that are analyzed here used a time step size of 10⁻⁴ second on 64×64×64 grid.

Figures 8 and 9 show the comparison of the liquid sloshing obtained from CFD simulation and experimental studies for two different time instance and liquid fill level. In figure 8, the first image is at the time of application of the brake. At this instance, the liquid surges towards the front end of the wall. The liquid surface contour from CFD compares well with the high speed video image. The second set of images in figure 8 is when the liquid sloshes back towards the rear wall. Here the slosh magnitude is higher than the first instance and liquid reaches the roof of the tank. The CFD captures well the increase in magnitude of the liquid wave height. As seen from figure 9, the sloshing magnitude for 60% fill level is less compared to the sloshing magnitude for 20% fill level. This is because, due to increased mass, the liquid has to overcome the larger initial inertial, which may be contributing to lower magnitude. However, when the liquid retraces to the rear of the tank, there is large air entrainment and the liquid surface becomes very bubbly. The surface profile from CFD is comparable to the images from high speed video.

To quantify the comparison between the CFD and experimental results, the difference between the liquid surface height obtained from CFD and experiment is compared and tabulated in tables 1 and 2. Several points were defined on the liquid surface and the ratio of interface height to distance from front wall is tabulated. This comparison is performed in the near linear sloshing regime because in the non-linear sloshing regime, there is large entrapment of bubbles which make the image interrogation for liquid surface very difficult. Error is define as, % Error = $(H_{CFD} - H_{Exp}) / H_{CFD} \times 100$. As can be seen from the tables, there are few locations where the percentage error between the CFD results and experimental measurements is large. However, a closer analysis reveals that these are occurring at locations that typically have low base values. Hence, even though the absolute difference may be small, the percentage error is large.

Table 1. Comparison between CFD and Experimental results for 20% fill level

Point	T = 1.3 sec			T = 1.75 sec		
	Exp.	Num.	% Error	Exp.	Num.	% Error
1	11.96	9.88	17.39	2.00	3.76	46.81
2	5.84	4.72	19.18	1.10	1.84	40.22
3	3.81	3.37	11.54	0.54	0.95	43.16
4	3.13	3.06	2.00	0.38	0.62	38.71
5	2.17	2.59	19.49	0.28	0.47	41.49
6	1.64	2.27	38.41	0.23	0.38	39.58
7	1.06	1.65	56.06	0.22	0.31	30.69
8	0.73	1.15	57.80	0.23	0.29	21.36
9	0.58	0.61	5.94	0.26	0.29	9.26
10	0.50	0.54	8.00	0.32	0.30	7.50
11	0.36	0.36	1.10	0.36	0.33	8.57
12	0.25	0.26	1.32	0.37	0.40	5.62
13	0.17	0.20	15.00	0.43	0.42	0.50
14	0.12	0.16	34.04	0.49	0.50	3.57
15	0.08	0.12	52.94	0.44	0.65	33.14
16	0.03	0.10	200.00	1.02	1.02	0.00

Table 2. Comparison between CFD and Experimental results for 60% fill level

Point	T = 1.3 sec			T = 1.75 sec		
	Exp.	Num.	% Error	Exp.	Num.	% Error
1	0.931	0.912	2.062	0.468	0.528	12.975
2	0.902	0.871	3.398	0.494	0.466	5.540
3	0.820	0.836	1.887	0.506	0.477	5.735
4	0.790	0.819	3.586	0.503	0.494	1.675
5	0.724	0.789	9.014	0.547	0.538	1.775
6	0.664	0.729	9.753	0.527	0.590	12.018
7	0.622	0.673	8.266	0.627	0.622	0.782
8	0.609	0.611	0.441	0.720	0.684	4.951
9	0.568	0.572	0.748	0.911	0.726	20.351
10	0.512	0.521	1.843	0.917	0.735	19.809
11	0.458	0.480	4.827	0.926	0.784	15.333
12	0.410	0.479	16.703			
13	0.351	0.490	39.661			

It must also be noted that the image interrogation technique presented here has a few sources of uncertainty: (a) liquid surface determination for bubbly flow is difficult to measure, (b)

liquid surface height is again difficult measure when the liquid height is small because meniscus effect due to wall wetting leads to uncertainty of surface location and (c) perspective projection of a 3D image on a 2D surface leads to parallax effects which may again lead to uncertainty in image interrogation. These uncertainties are higher in non-linear flow regime and subsequently decrease in the linear slosh regime. Hence the measurements presented in the two tables are at time instances when the flow is in the linear flow regime.

Acoustic Simulation

Numerical analysis has been done in accordance to the flowchart discussed in [Figure 4](#) using commercial software LMS Virtual. Lab. The calculated total sound pressure level (SPL) results are in good agreement with experimental results. [Figure 10](#) shows the sound pressure spectrum for 20% and 60 % liquid fill level in the tank at the field points. The chosen field point locations are same as microphones used in the experimental setup. These results generated based on frequency approach. The peak SPL for 20 % fill level in experiments is 77 dB and predicted total SPL is 75 dB and 60% fill level 77 dB in experiment and 70 dB in simulation. There is a good correlation between experiment and simulation results for 20% fill but it is not true for 60 % fill level. The main reasons for the discrepancy between experiment and simulation for 60% fill level are non-linear sloshing and also the dominance of splash noise. The proposed frequency domain prediction model is good for linear sloshing and also hit noise prediction but not for splash noise.

Conclusion

In the present paper, an integrated VOF based multiphase CFD model, Finite element and boundary element models have been applied to the numerical simulation of liquid sloshing noise from a rectangular tank. The proposed simulation results have been compared with the existing literature and experimental data.

Experimental test setup has been developed to measure liquid sloshing noise under control loading. In the experiment, a rectangular tank was subjected to a breaking load in the vehicle moving direction. Different sensors have been used to monitor the dynamic force and acceleration on the outer tank wall surface, and sound pressure level around the tank. The following conclusions can be obtained based on experimental and simulation results. Firstly, there is a direct correlation between all the sensor data and also major sloshing events. The interval duration between successive sloshing events was same as sloshing natural period for linear sloshing. Secondly, with the increasing fill level, sloshing becomes non-linear. The sloshing period between two successive events was not the same. Simulation results deviated from experimental results for non-linear sloshing. The assumption of insignificant change in liquid CG location is not valid for non-linear sloshing. So, further work is required to improve the prediction accuracy in the non-linear sloshing region, which should be based on time-domain approach. Thirdly, CFD simulation results, especially in the linear sloshing region have been corroborated

with liquid sloshing wave heights captured using high speed camera in the experiment. Lastly, the proposed simulation algorithm under predict sloshing noise compared to experimental results because it can capture only hit noise but not splash and clank noise. However, the experimental setup can capture total sloshing noise.

References

1. Wachowski, C., Biermann, J.-W., and Schala, R., "Approaches to Analyse and Predict SLOSH Noise of Vehicle Fuel Tanks," *Proceedings of ISMA2010 Including USD2010*, 2010.
2. aus der Wiesche S., "Noise due to sloshing within automotive fuel tanks," *Forsch. im Ingenieurwes.*, vol. 70, no. 1, pp. 13-24, Nov. 2005.
3. Kamei, M., Hanai, J., Fukasawa, W., and Makino, T., "Establishment of a Method for Predicting and Confirming Fuel Tank Sloshing Noise," SAE Technical Paper [2007-01-1538](#), 2007, doi:[10.4271/2007-01-1538](#).
4. Stednitz, W. and Appel, H., "Experimental And Analytical Simulation Of Liquid Sloshing In Tank TrucksFigs, 1," SAE Technical Paper [885110](#), 1988, doi:[10.4271/885110](#).
5. Kamiya, K., Yamaguchi, Y., and de Vries, E., "Simulation Studies of Sloshing in a Fuel Tank," SAE Technical Paper [2002-01-0574](#), 2002, doi:[10.4271/2002-01-0574](#).
6. IU, H., Cleghorn, W., and Mills, J., "Design and Analysis of Fuel Tank Baffles to Reduce the Noise Generated From Fuel Sloshing," SAE Technical Paper [2004-01-0403](#), 2004, doi:[10.4271/2004-01-0403](#).
7. Roh, W., Cho, S., and Park, J., "Simulation of Sloshing in Fuel Tanks and Parametric Study on Noise Reduction by Decreasing Impact Pressure," SAE Technical Paper [2005-01-1913](#), 2005, doi:[10.4271/2005-01-1913](#).
8. Di Matteo, L., Fortunato, F., Oliva, P., Fiore, N. et al., "Sloshing Analysis of an Automotive Fuel Tank," SAE Technical Paper [2006-01-1006](#), 2006, doi:[10.4271/2006-01-1006](#).
9. Wasfy, T., O'Kins, J., and Smith, S., "Experimental Validation of a Time-Accurate Finite Element Model for Coupled Multibody Dynamics and Liquid Sloshing," SAE Technical Paper [2007-01-0139](#), 2007, doi:[10.4271/2007-01-0139](#).
10. Chitkara, T., Kittur, Z., and Soman, R., "Computational Simulation of Fuel Tank Sloshing using CFD Techniques," SAE Technical Paper [2013-01-2868](#), 2013.
11. De Man, P. and Van Schaftingen, J., "Prediction of Vehicle Fuel Tank SLOSH Noise from Component-Level Test Data," SAE Technical Paper [2012-01-0215](#), 2012, doi:[10.4271/2012-01-0215](#).
12. Li, F., Sibal, S., McGann, I., and Hallez, R., "Radiated Fuel Tank SLOSH Noise Simulation," SAE Technical Paper [2011-01-0495](#), 2011, doi:[10.4271/2011-01-0495](#).
13. Park, J., Choi, S., and Hong, S., "The Prediction of Fuel Sloshing Noise Based on Fluid-Structure Interaction Analysis," *SAE Int. J. Passeng. Cars - Mech. Syst.* 4(2):1304-1310, 2011, doi:[10.4271/2011-01-1695](#).
14. Vytla, V. and Ando, Y., "Fluid Structure Interaction Simulation of Fuel Tank Sloshing," SAE Technical Paper [2013-01-0641](#), 2013, doi:[10.4271/2013-01-0641](#).
15. Star CCM+ Users's Guide, CD Adapco, 2011
16. LMS Virtual Lab, User's Manual, LMS International, 2012

Contact Information

Corresponding author:

R. Banerjee

Ph: +91-40-2301-6015

rajabanerjee@iith.ac.in

Acknowledgments

The authors would like to acknowledge the financial support of Mercedes Benz India Pvt. Ltd. for this work.

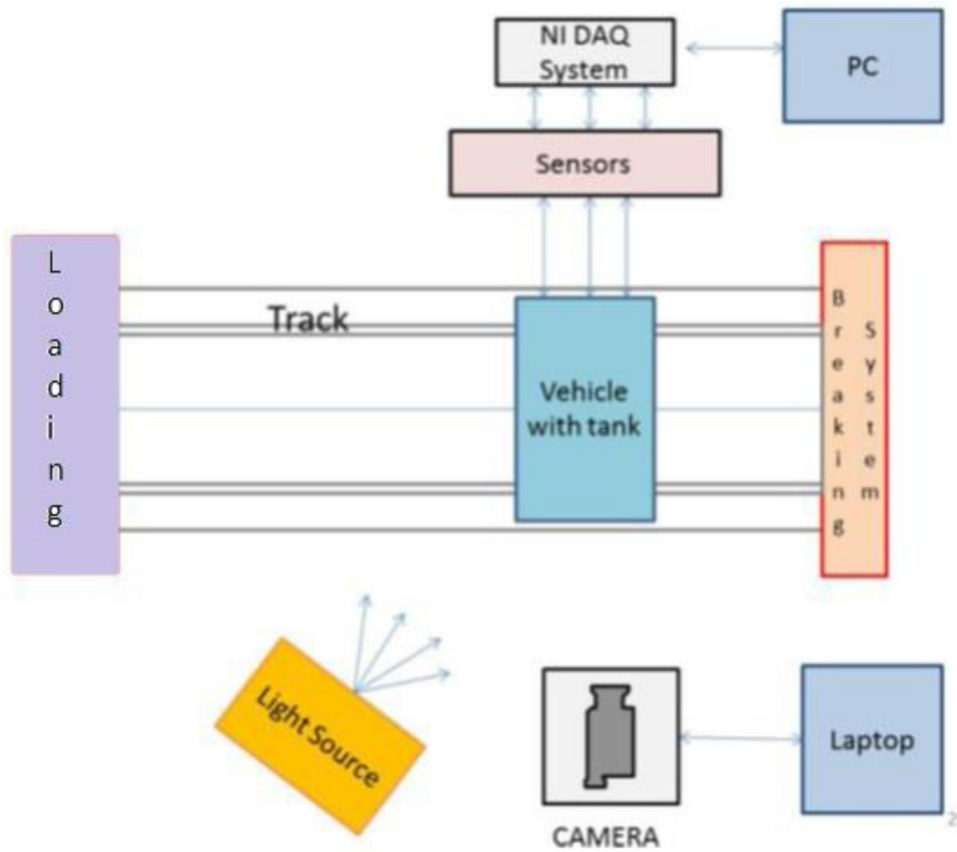


Figure 1. Schematic of the Experimental Setup

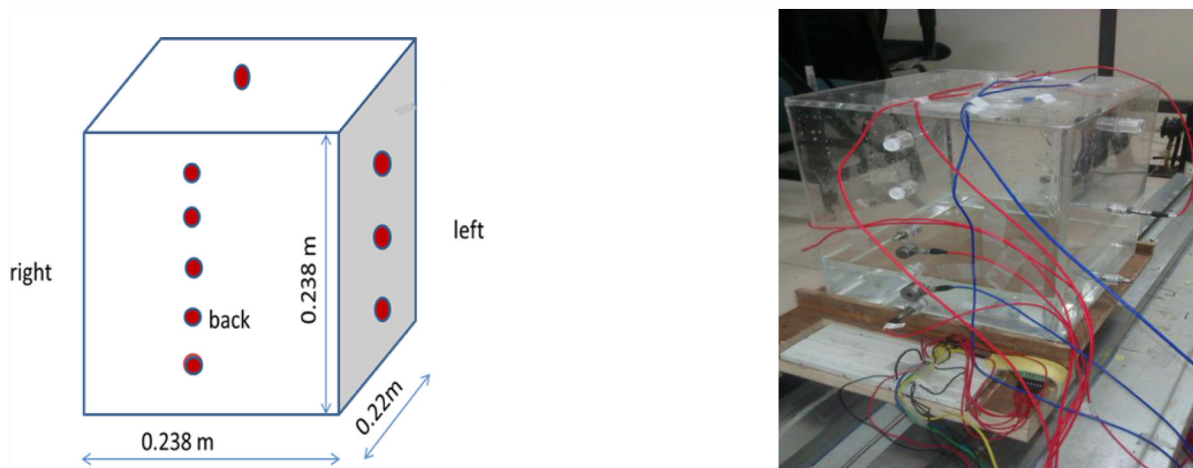


Figure 2. Transparent rectangular tank with sensor mounting positions

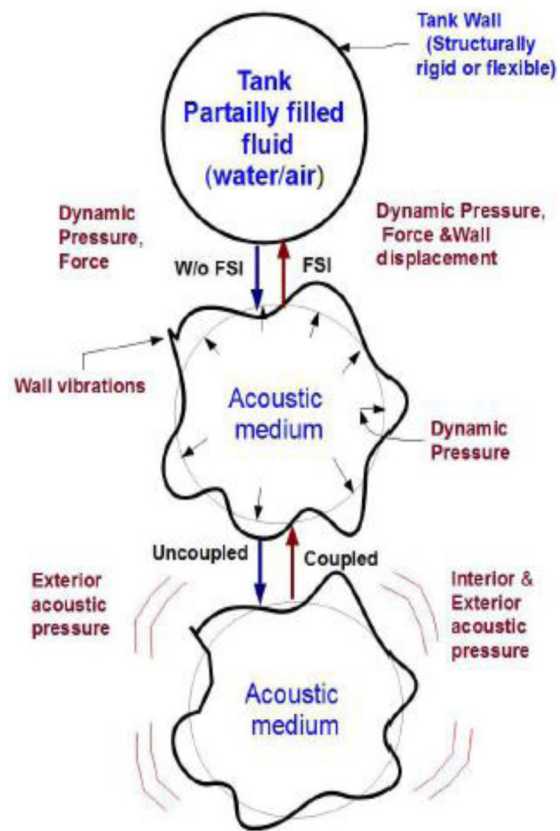


Figure 3. Philosophy of sloshing noise simulation

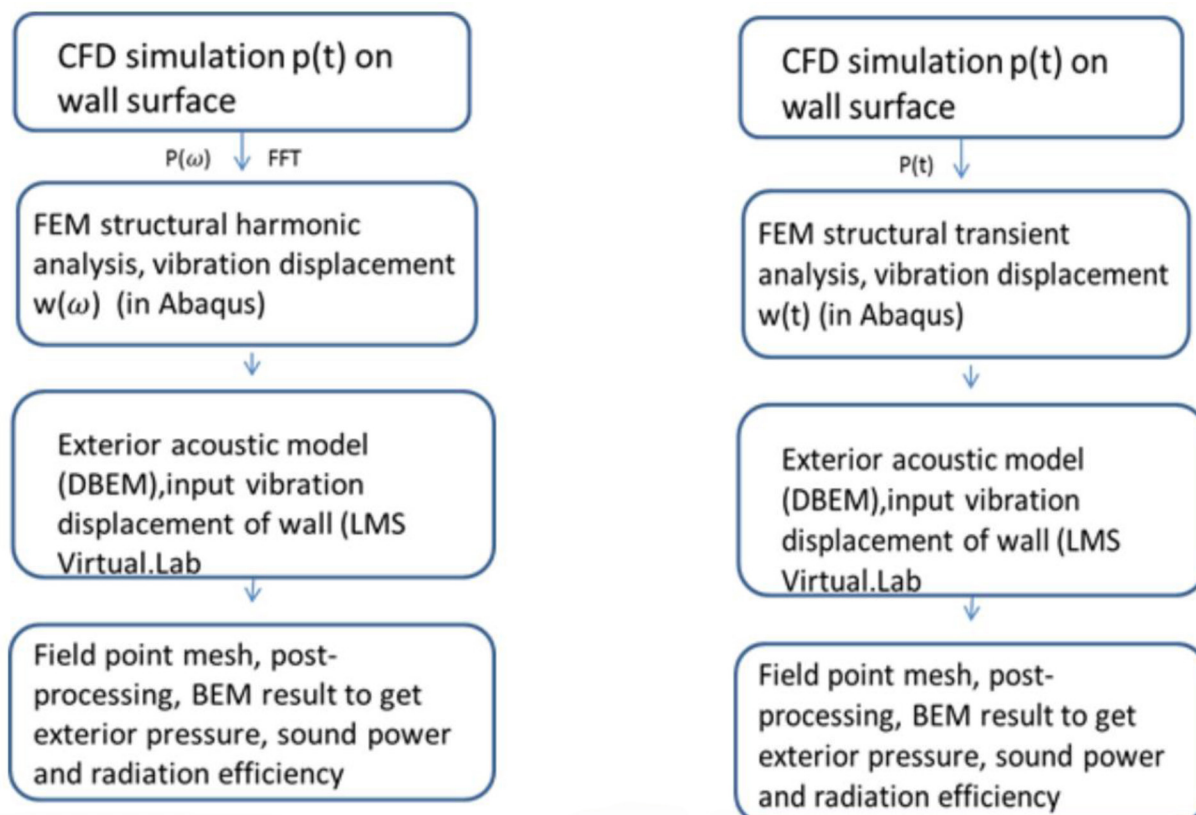


Figure 4. Uncoupled approach for vibro-acoustic simulation modelling (a) frequency domain approach (b) time domain approach

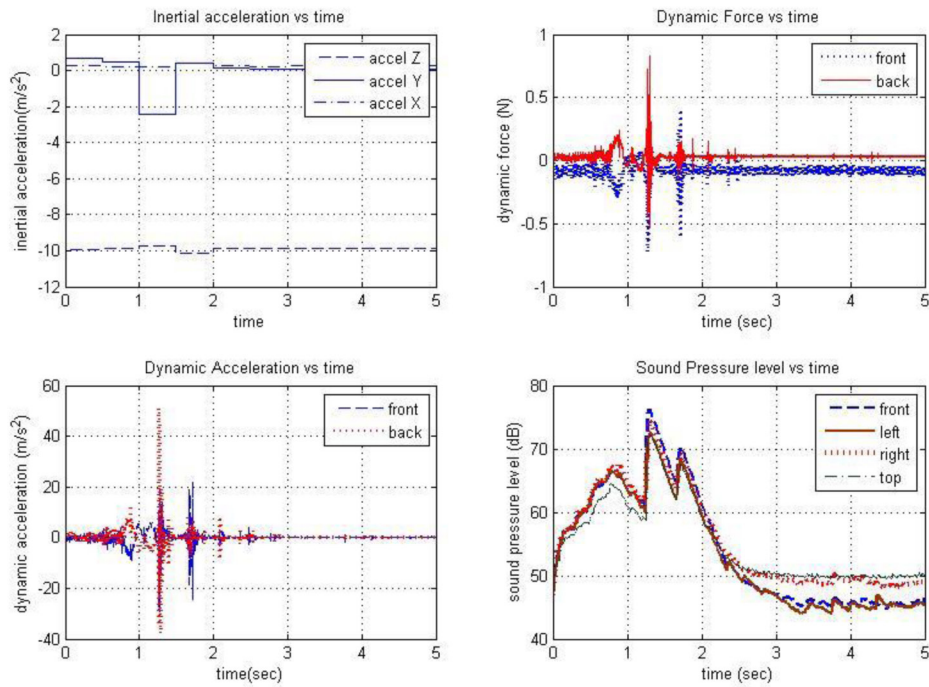


Figure 5. Experimental results for 20% fill level (a) Inertial acceleration (b) Dynamic force (c) Dynamic acceleration (d) Sound pressure level

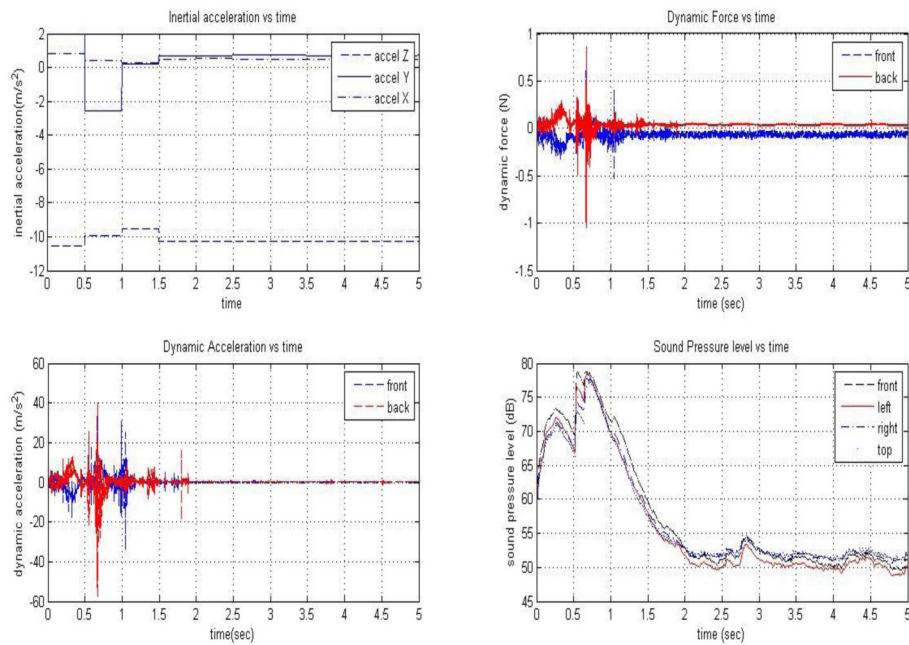


Figure 6. Experimental results for 60% fill level (a) Inertial acceleration (b) Dynamic force (c) Dynamic acceleration (d) Sound pressure level

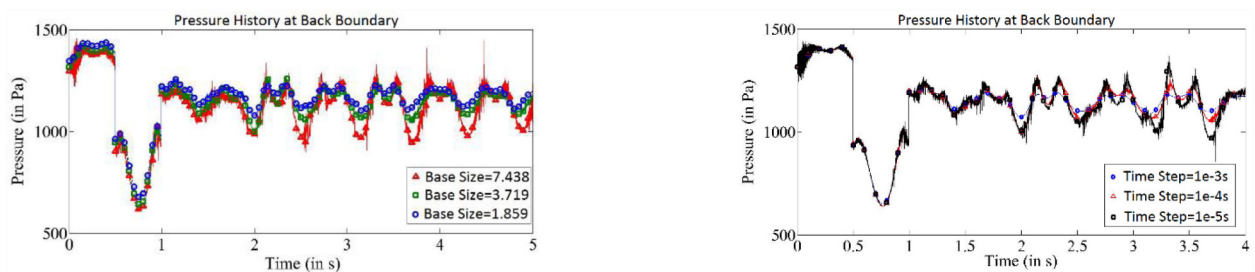


Figure 7. Grid and time independence study for CFD

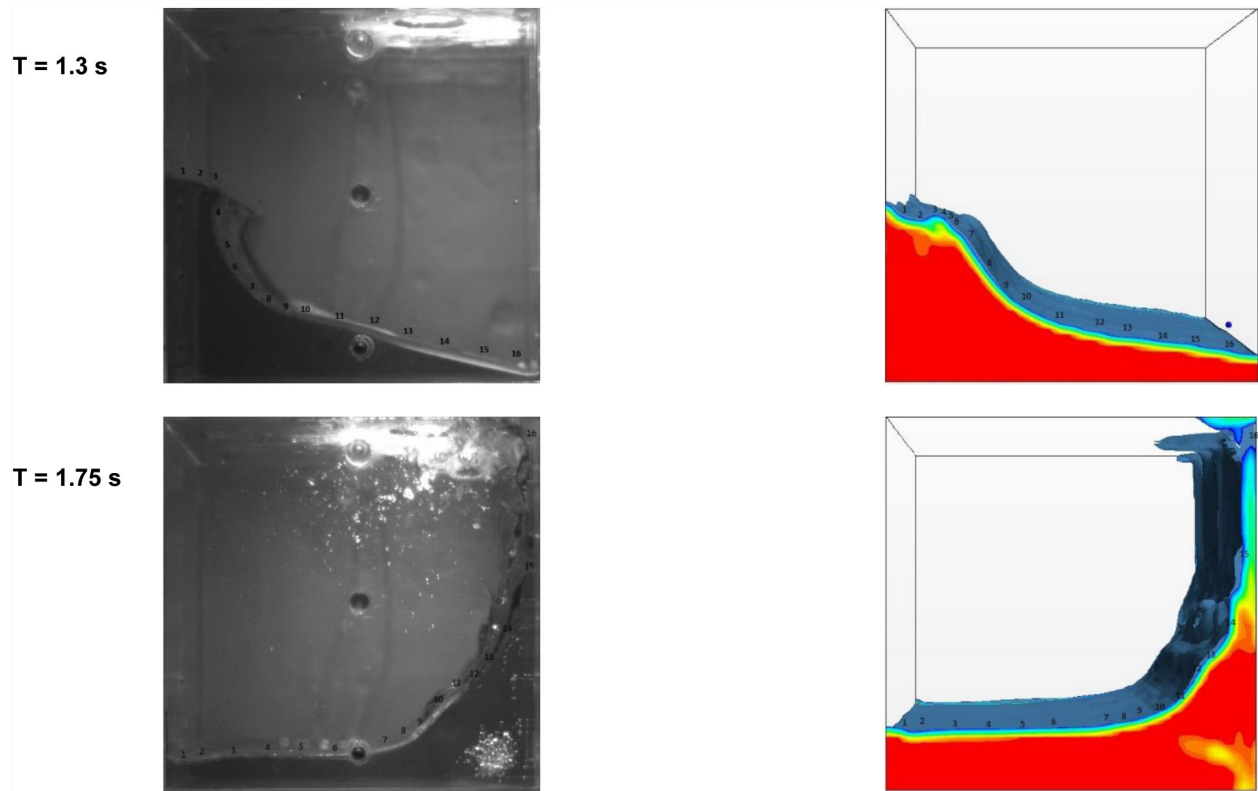


Figure 8. Comparison between experiment and CFD results for 20% fill level

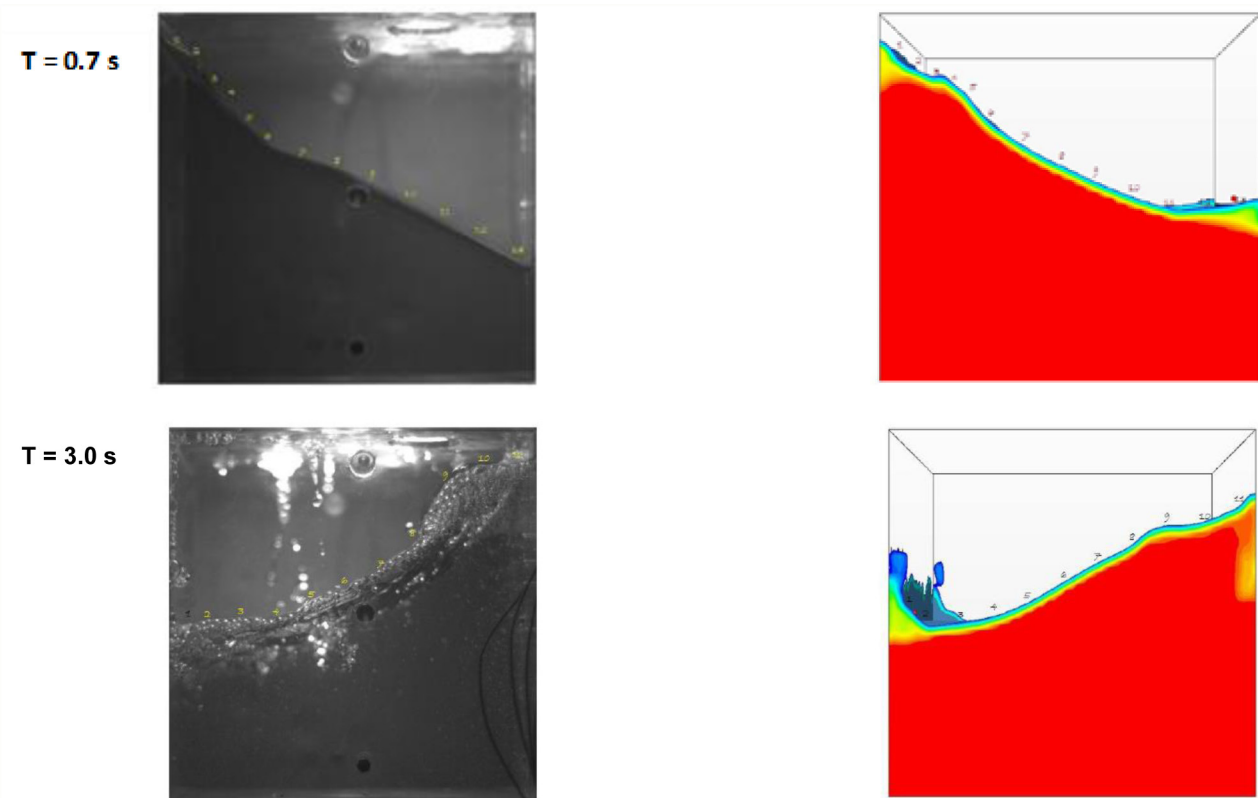


Figure 9. Comparison between experiment and CFD results for 60% fill level

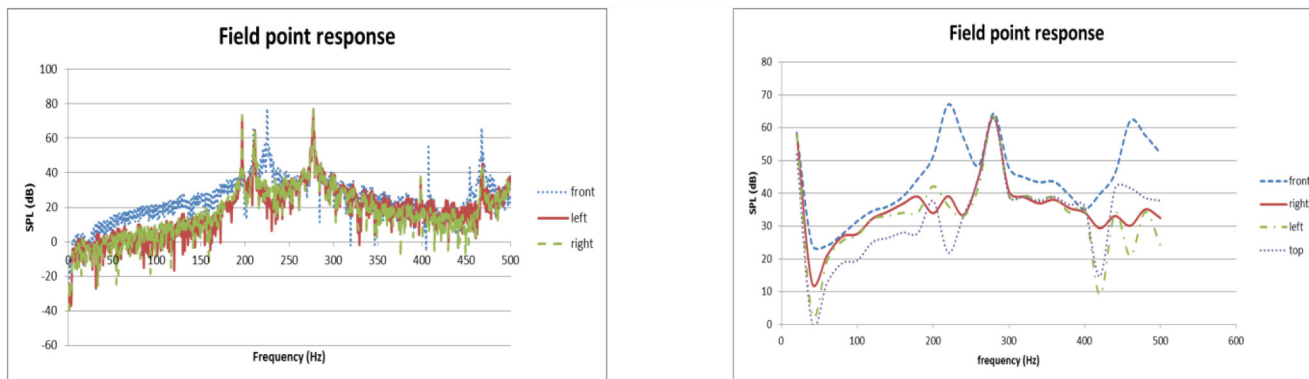


Figure 10. Prediction of sound pressure spectrum from LMS (a) 20% tank fill (b) 60% tank fill

The Engineering Meetings Board has approved this paper for publication. It has successfully completed SAE's peer review process under the supervision of the session organizer. The process requires a minimum of three (3) reviews by industry experts.

All rights reserved. No part of this publication may be reproduced, stored in a retrieval system, or transmitted, in any form or by any means, electronic, mechanical, photocopying, recording, or otherwise, without the prior written permission of SAE International.

Positions and opinions advanced in this paper are those of the author(s) and not necessarily those of SAE International. The author is solely responsible for the content of the paper.